Photoacoustics 31 (2023) 100514

Contents lists available at ScienceDirect

Photoacoustics

journal homepage: www.elsevier.com/locate/pacs

Longitudinal volumetric assessment of inflammatory arthritis via photoacoustic imaging and Doppler ultrasound imaging

Xiaorui Peng [a], Zhanpeng Xu [a], Aaron Dentinger [b], Shivangi Kewalramani [a], Janggun Jo [a], Guan Xu [a,c], David Chamberland [d], Nada Abdulaziz [d,*], Girish Gandikota [e,*], David Mills [b,*], Xueding Wang [a,e,**]

[a] Department of Biomedical Engineering, University of Michigan, Ann Arbor, MI, USA
[b] General Electric Research, Niskayuna, NY, USA
[c] Department of Ophthalmology and Visual Sciences, University of Michigan, Ann Arbor, MI, USA
[d] Division of Rheumatology, Department of Internal Medicine, University of Michigan, Ann Arbor, MI, USA
[e] Department of Radiology, University of Michigan, Ann Arbor, MI, USA

ARTICLE INFO

Keywords:
Rheumatoid arthritis
Photoacoustic imaging
Doppler ultrasound imaging
Three-dimensional imaging
Early diagnosis

ABSTRACT

Aiming at clinical translation, we developed an automatic 3D imaging system combining the emerging photoacoustic imaging with conventional Doppler ultrasound for detecting inflammatory arthritis. This system was built with a GE HealthCare (GEHC) Vivid™ E95 ultrasound system and a Universal Robot UR3 robotic arm. In this work, the performance of this system was examined with a longitudinal study utilizing a clinically relevant adjuvant induced arthritis (AIA) murine model. After adjuvant injection, daily imaging of the rat ankle joints was conducted until joint inflammation was obvious based on visual inspection. Processed imaging results and statistical analyses indicated that both the hyperemia (enhanced blood volume) detected by photoacoustic imaging and the enhanced blood flow detected by Doppler ultrasound reflected the progress of joint inflammation. However, photoacoustic imaging, by leveraging the highly sensitive optical contrast, detected inflammation earlier than Doppler ultrasound, and also showed changes that are more statistically significant. This side-by-side comparison between photoacoustic imaging and Doppler ultrasound using the same commercial grade GEHC ultrasound machine demonstrates the advantage and potential value of the emerging photoacoustic imaging for rheumatology clinical care of arthritis.

1. Introduction

Rheumatoid arthritis (RA) is a chronic systemic autoimmune disease that often leads to bone erosion, articular cartilage damage, and tendon tears [1–4]. RA affects approximately 1 % of the world's population and can cause disability and consequential inability to work [5]. The metacarpophalangeal (MCP) and proximal interphalangeal (PIP) joints are the most affected joints in RA [6]. Early diagnosis of RA is of great clinical importance as it enables clinicians to execute the treatment plan before substantial irreversible joint damage occurs [7].

Magnetic resonance imaging (MRI) and ultrasound (US) imaging can both be used in the early detection of inflammation [8]. In current clinic, rheumatologists use gadolinium-enhanced MRI or Doppler sonography to confirm the presence of joint inflammation [5]. MRI is often used as the reference standard for assessing the accuracy of US detection of RA [9] due to the high-level agreement with pathologic findings [10–12]. However, the disadvantages of MRI include limited accessibility, long imaging time, financial constraints, and potential contraindications [6]. US imaging is more often used in clinical assessment of RA due to its advantages in terms of availability, accuracy, image resolution, and cost [13–15]. However, US imaging has a significant learning curve for inexperienced operators, and its assessment is also highly dependent on the operator [6].

Recently, photoacoustic (PA) imaging, with intrinsically high sensitivity to hemoglobin in blood vessels, emerged as a potential tool for detecting and grading soft-tissue inflammation associated with arthritis [16–20]. Experiments on RA patients confirmed that PA imaging can map spatially distributed hyperemia (increased blood volume) and

* Corresponding authors.
** Corresponding author at: Department of Biomedical Engineering, University of Michigan, Ann Arbor, MI, USA.
E-mail addresses: nabdulaz@med.umich.edu (N. Abdulaziz), ggirish@med.umich.edu (G. Gandikota), millsda@ge.com (D. Mills), xdwang@umich.edu (X. Wang).

https://doi.org/10.1016/j.pacs.2023.100514
Received 3 February 2023; Received in revised form 26 April 2023; Accepted 20 May 2023
Available online 21 May 2023

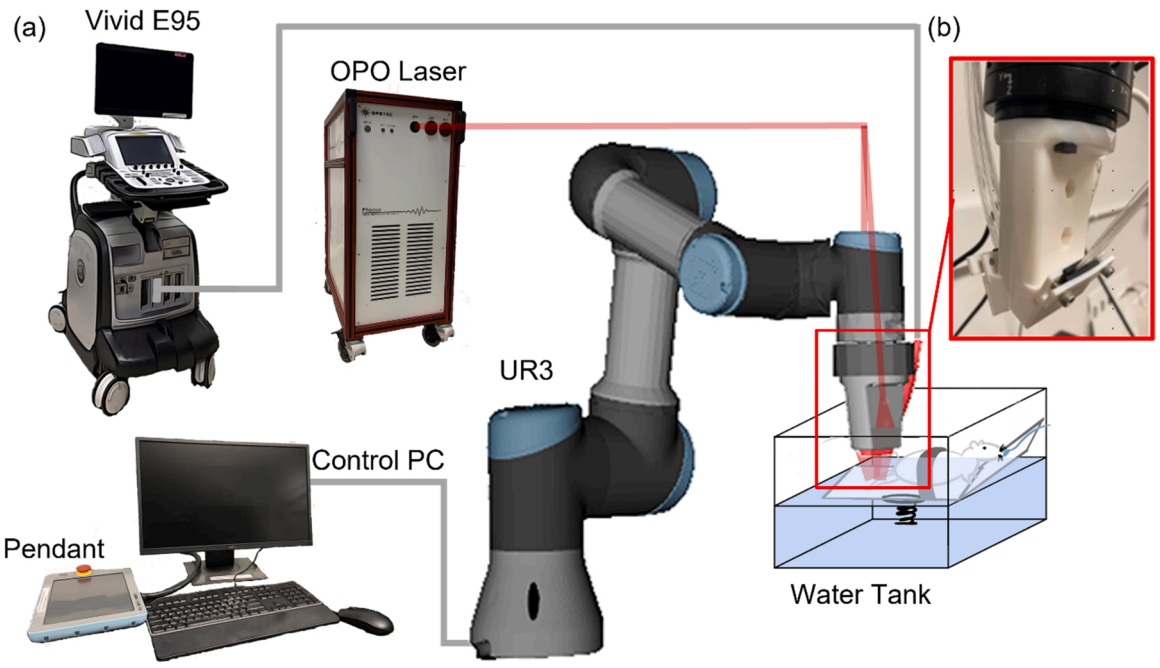

Fig. 1. (a) Automatic 3D PA and Doppler US multi-modality imaging system configuration. (b) Photo of the imaging probe holder with a L8–18i-D probe in the middle and two fiber bundles at the two sides.

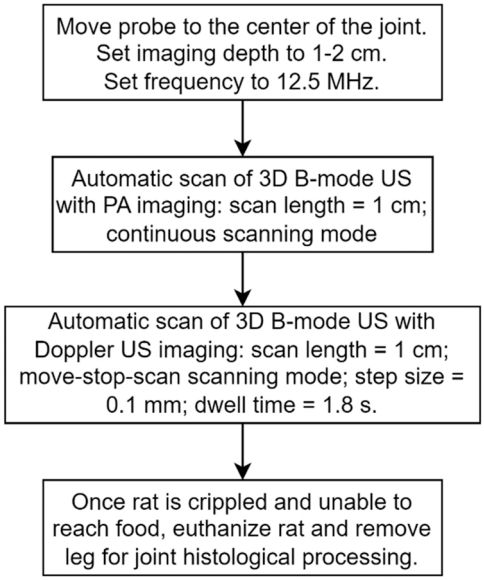

Fig. 2. Daily imaging procedure.

hypoxia (decreased blood oxygenation) as two imaging biomarkers reflecting soft-tissue inflammation [16]. In another study involving a larger cohort of 118 RA patients, Yang et al. validated that the hypoxia detected by PA imaging in thickened synovium correlates with less vascularization and higher disease activity [20]. In a study involving both an LED-based PA imaging system and a commercial US system, the sensitivity of PA imaging vs Doppler US in detecting joint inflammation were compared, and PA imaging showed higher sensitivity in detecting mild inflammation in patients with sub-clinically active arthritis [21]. The findings from these pioneering clinical studies are encouraging and suggest that PA imaging holds potential as a new tool for clinical care of arthritis in rheumatology.

Besides clinical studies in RA patients, the feasibility of PA imaging for evaluating joint inflammation has also been explored in animal models of arthritis [22–28]. Compared to human patients, animal models, especially murine models, develop arthritis much faster and hence, can facilitate studies of longitudinal imaging of these pathological conditions and their responses to treatment within shorter time periods. Studies using large numbers of these murine models for statistical significance also benefit from the low costs of these models. In addition, studies that use animal models allow validation of findings from imaging with histopathology as the gold standard which is typically not practical in large numbers with human patients. With these advantages, animal models of arthritis offer well-controlled platforms for objectively and comprehensively assessing the performance and understanding the limitations of the emerging PA imaging technique.

Aiming at clinical translation, we recently developed an automatic 3D PA and Doppler US multi-modal imaging system for detecting inflammatory arthritis. This system was built on a commercial-grade GE HealthCare (GEHC) Vivid™ E95 (VE95) US system and a Universal Robot UR3 robotic arm. In this work, the performance of this system was examined in a longitudinal study utilizing a clinically relevant adjuvant induced arthritis (AIA) murine model. Among all the models that we have investigated for human inflammatory diseases, the AIA rat model is one of the best, not only because it is similar clinically and histopathologically to human RA but also due to its good consistency [22,23,29–31]. In the AIA model, 90–100 % of rats develop arthritis within 20 days after adjuvant injection, showing joint histological changes including leukocyte invasion preceding joint swelling [32]. In this study, the rat ankle joints were imaged daily after adjuvant injection by using our automatic 3D multi-modal imaging system. Longitudinal progress of inflammation in rat ankle joints were quantitatively evaluated by both PA imaging and power Doppler US imaging. This side-by-side comparison between the two modalities, realized by the same commercial grade US system, allowed us to objectively assess the advantages and limitations of the emerging PA imaging technique and benchmark it against conventional Doppler US.

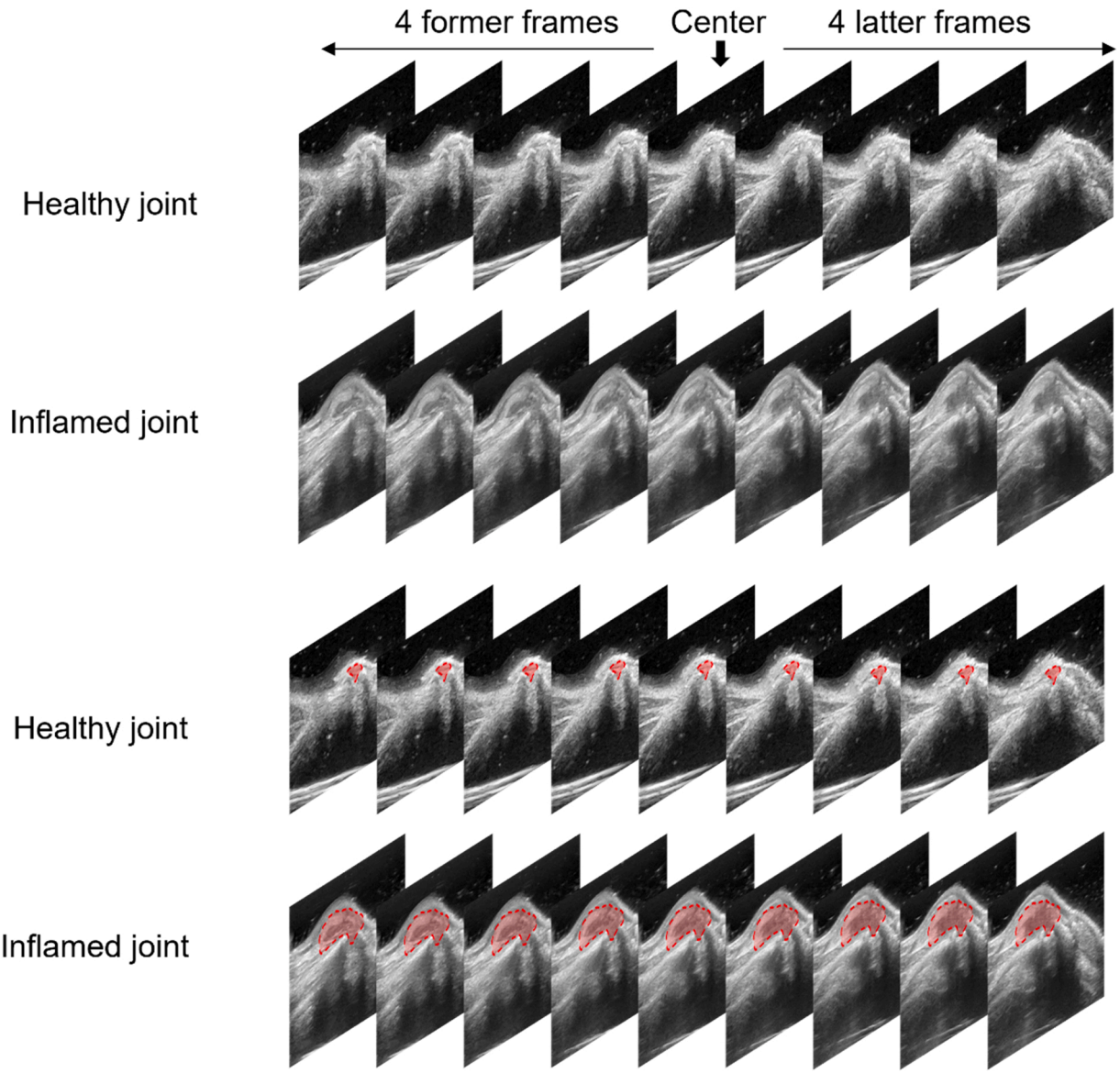

Fig. 3. Example 3D B-mode US images from a healthy joint (first row) and an inflamed joint (second row), 9 frames each (center frame to +/- 4 frames). Manual segmentation of the synovial tissue and the adjacent region in the healthy joint (third row) and the inflamed joint (fourth row). The segmented areas are marked by red dashed lines and shadows. (For interpretation of the references to color in this figure legend, the reader is referred to the web version of this article.)

2. Methods

2.1. Imaging system

The automatic 3D PA and Doppler US multi-modality imaging system setup is shown in Fig. 1(a). This system, based on a GEHC VE95 US unit and a GEHC L8–18i-D high-frequency linear probe, can simultaneously acquire B-mode US images and PA images in real time. The customized probe holder, as shown in Fig. 1(b), which held an US linear array probe in the middle and two fiber bundles at the two sides, was attached to a Universal Robots UR3 robotic arm. We used an Nd:YAG pumped OPO (Phocus MOBILE, OPOTEK, Carlsbad, CA) with repetition rate of 10 Hz, wavelength tuning range of 690–950 nm, and pulse length of 5 ns as the light source for PA imaging. In this study, laser pulses at a single wavelength of 750 nm with a pulse energy of 40 mJ were applied to an illumination area of 2 cm^2 on the target joint, leading to pulse energy density of 20 mJ/cm^2 which was within the ANSI safety limit. The output end of the fiber bundle at the two sides of the probe was placed at a 30-degree angle to achieve the optimal light fluence and penetration depth. The 168-element GEHC L8–18i-D probe worked at 12.5 MHz center frequency for both PA and US signal detection.

The proprietary software on the GE VE95 US system was modified to provide the new functionality for the PA imaging mode. We configured the VE95 US unit to receive a trigger from the tunable laser to start the receive chain without a transmit event from the US unit. By modifying the VE95's signal processing capability for this one-way ultrasound propagation, we could create an image using the received PA signals following a single laser pulse illumination. We also interleaved B-mode US imaging pulses between each PA laser firing to provide a structural image and facilitate the spatial registration of these two modalities. Both PA images and B-mode US images were acquired, stored, and displayed on the VE95 in real time. The VE95 US system also performed color or power Doppler US imaging.

To achieve 3D imaging of a joint, the probe held by the robotic system automatically scanned along the determined scanning path and enabled volumetric reconstruction in post-processing. The robotic arm was controlled by the control PC with a user interface (UI) that we developed. In the PA acquisition mode, the probe continuously scanned

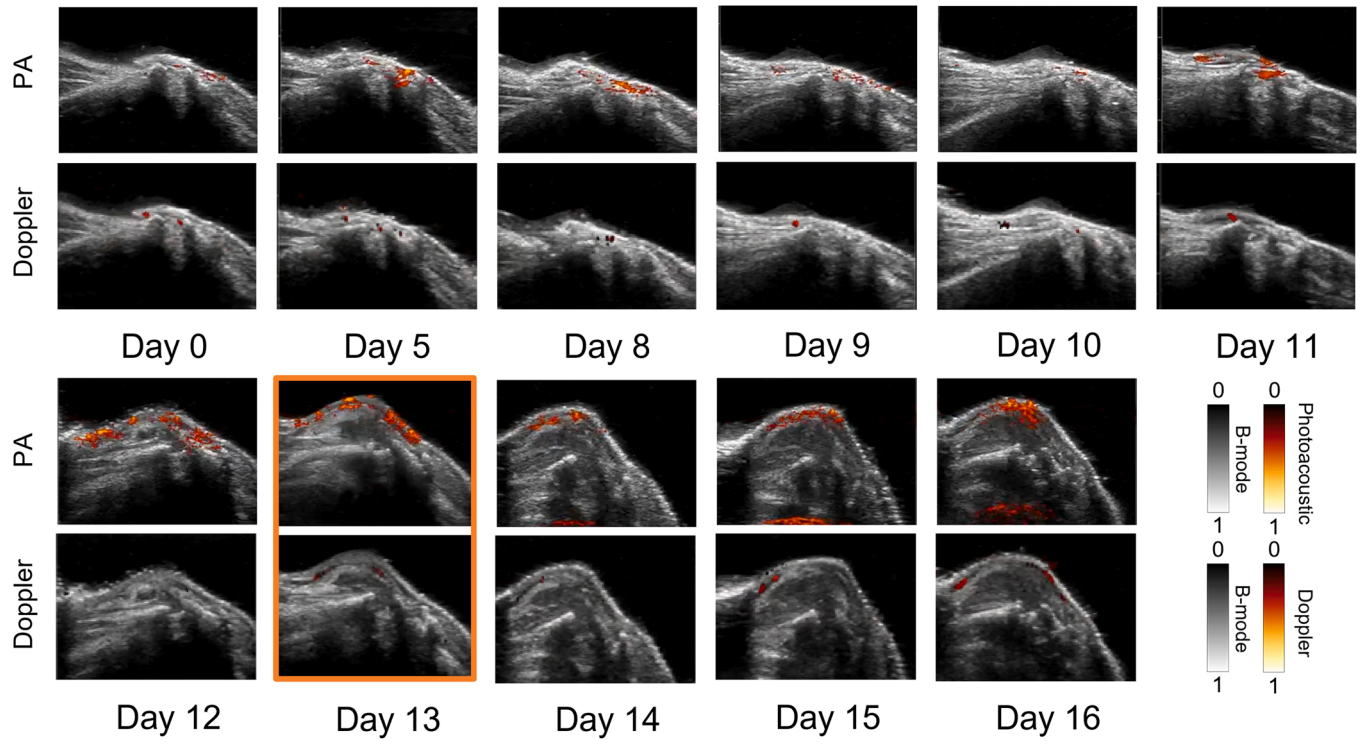

Fig. 4. Longitudinal imaging of inflammation in the right ankle joint of an AIA rat, including the imaging before AIA injection (Day 0) and at different time points after the AIA injection. PA images superimposed on the B-mode US images are compared to power Doppler US images superimposed on the B-mode US images.

from one side of the joint to the other side. In the Doppler US mode, the probe utilized a move-stop-scan approach which allowed it to dwell for a short period of time to avoid motion artifacts in the Doppler images and then moved to the next location, stopped, and scanned images. PA and power Doppler US images were formed using delay-and-sum algorithms and represented by normalized pseudo colors and superimposed on 3D B-mode US images. The resolution for both long-axis and reconstructed short-axis B-mode US imaging was adequate for 3D rendering of the whole joint.

2.2. Adjuvant induced arthritis (AIA) rat model

All experimental animal procedures were approved by the Institutional Animal Care & Use Committee (IACUC) of the University of Michigan (Animal protocol: PRO00009524). Seven female rats (Sprague Dawley, 5–6 weeks age, Envigo, Indianapolis, IN) were used for the study. Before inducing AIA, each animal was anesthetized with isoflurane using an induction box and then maintained on isoflurane via a mask. The AIA was introduced by injecting a mixture of lyophilized Mycobacterium butyricum (powdered form, H37 Ra, Difco Labs, Detroit, MI) and mineral oil (Paraffin oil, Fisher Scientific, Hampton, NH) to the base of the rat's tail. To prepare the mixture, powdered Mycobacterium butyricum (15 mg) was added to 2 ml of mineral oil and ground in a mortar and pestle for thirty minutes. For each rat, 0.4 ml of the mixture was injected into the base of the tail under aseptic conditions.

2.3. Imaging procedure

Right before (Day 0 as the baseline) and after adjuvant injection, daily imaging of the rat ankle joint was conducted until the animal was euthanized. The total time duration for daily imaging after adjuvant injection ranged from 9 days to 21 days. This was because the animals have individual difference in time when responding to the AIA injection. When the systemic inflammation became very serious, the animal's joints would be extremely swollen and stiff. At this time point, the animal was crippled and unable to reach food, and had to be euthanized by following the protocol approved by the IACUC of the University of Michigan.

The daily scanning procedure is shown in Fig. 2. All 14 ankle joints of the 7 rats were imaged. For each imaging procedure, the rat was anesthetized with an isoflurane anesthesia system attached to a mask and placed on an adjustable height stage in a water tank. The target ankle joint for imaging was submerged in the warm water with a constant temperature of 37 °C.

When imaging each joint, the robotic arm moved the probe to the target joint. The probe aligned with the joint along the sagittal view and stopped at the location where the ankle joint structure could be visualized clearly by the B-mode US. The distance between the probe and the ankle was approximately 1–2 cm which is the range with the best image quality for the GEHC L8–18i-D array. We used the designed user interface to adjust scanning parameters including imaging mode, scan length, continuous scan mode or move-stop-scan mode, step size of every movement and dwell time. Then, 3D B-mode US together with PA imaging was performed by scanning the probe over a 1-cm distance across the joint, following the continuous scanning mode. The continuous scan of each 3D B-mode US image together with the PA image took 7.4 s, acquiring 135 frames in total. After that, 3D B-mode US together with power Doppler US imaging was performed on the same joint, following the move-stop-scan scanning mode. Covering the same 1-cm scanning distance with a 0.1 mm step size and 1.8 s dwell time, the scan of each 3D B-mode US image together with the Doppler US image took 180 s, acquiring 99 frames in total. At the end of the longitudinal daily imaging study, each rat was euthanized and both legs were harvested for histology analysis.

2.4. Histology examination

To confirm joint inflammation induced by adjuvant injection as well as imaging findings, Hematoxylin and Eosin (H&E) staining histology of

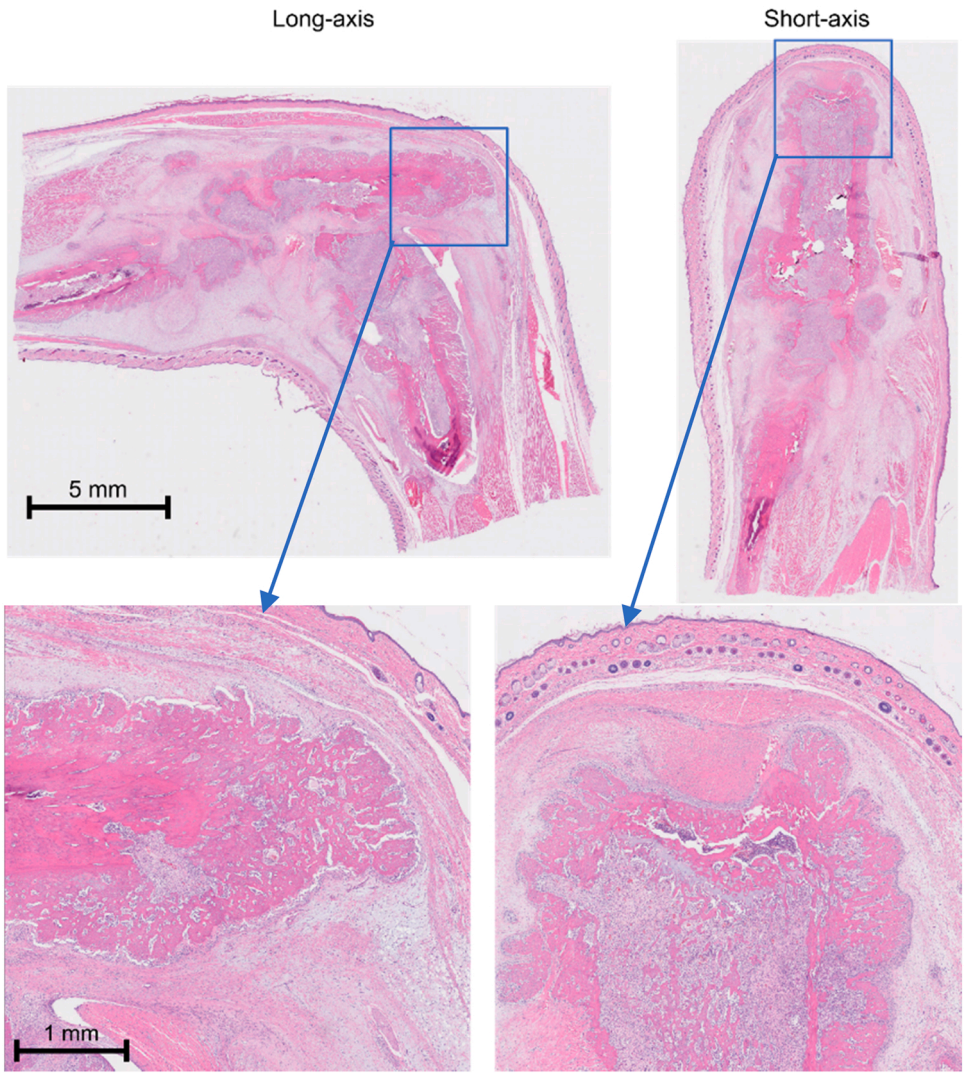

Fig. 5. H&E-stained histology photos taken along the long-axis of the right ankle joint and the short-axis of the left ankle joint of the same rat with the imaging results shown in Fig. 4. The detailed synovial tissue hyperplasia areas are marked in blue boxed and also shown with larger magnification. (For interpretation of the references to color in this figure legend, the reader is referred to the web version of this article.)

the affected ankle joints was conducted at the University of Michigan In-Vivo Animal Core (IVAC). H&E staining is suitable for quantification of synovial inflammation and detection of cartilage and bone erosions [33, 34]. For each animal at the end of the longitudinal imaging study, both legs were removed and fixed in 4 % Parafomaldehyde. One of the fixed legs was cut into longitudinally trimmed slices, while the other leg was cut into cross-sectionally trimmed slices. The slices were then scanned with a Polaris brightfield digital scanner and analyzed using the Aperio ImageScope software (Leica Biosystems, Wetzlar, Germany).

2.5. Image segmentation and quantitative analysis

We manually segmented the synovial tissue and the adjacent region, including muscle and tendon, in the center frame of the B-mode US images acquired from each joint. The segmentation was performed using the center frame because this frame presented the best image of the ankle joint structure. We then applied the same segmentation mask to the former and the latter 4 adjacent frames, with 9 frames in total, as shown in Fig. 3. These 9 segmented frames form the target volume for assessment of joint inflammation. For quantitative analysis of the hyperemia (enhanced blood volume) in the joint, we calculated the total intensity of the color pixels and the total number of color pixels in the target volume using the PA and Doppler US images. These quantitative measurements were evaluated to determine if they reflect the severity of disease in the synovial tissue and surrounding region.

3. Results

A representative result from the longitudinal imaging study of a rat's right ankle joint affected by AIA is shown in Fig. 4, which includes the images acquired before the AIA injection (Day 0) and at Day 5, 8, 9, 10, 11, 12, 13, 14, 15, and 16 after the injection. The gray-scale B-mode US images with superimposed PA signals in pseudo color are compared with the gray-scale B-mode US images with superimposed power Doppler US signals. The joint morphologies presented by the B-mode US images acquired respectively with the PA mode and the power Doppler US mode are similar, demonstrating that the image acquisition driven by the robot is robust and stable. To benefit comparison, the pixel intensities in the PA images and the power Doppler US images are displayed using the same colormap.

In this joint, no sign of inflammation was visible until Day 12. Then, the joint started appeared swollen due to the proliferation of the joint capsule and the swelling progressed rapidly from Day 12 to Day 16. On Day 16, the rat legs were very swollen and stiff, making the rat crippled.

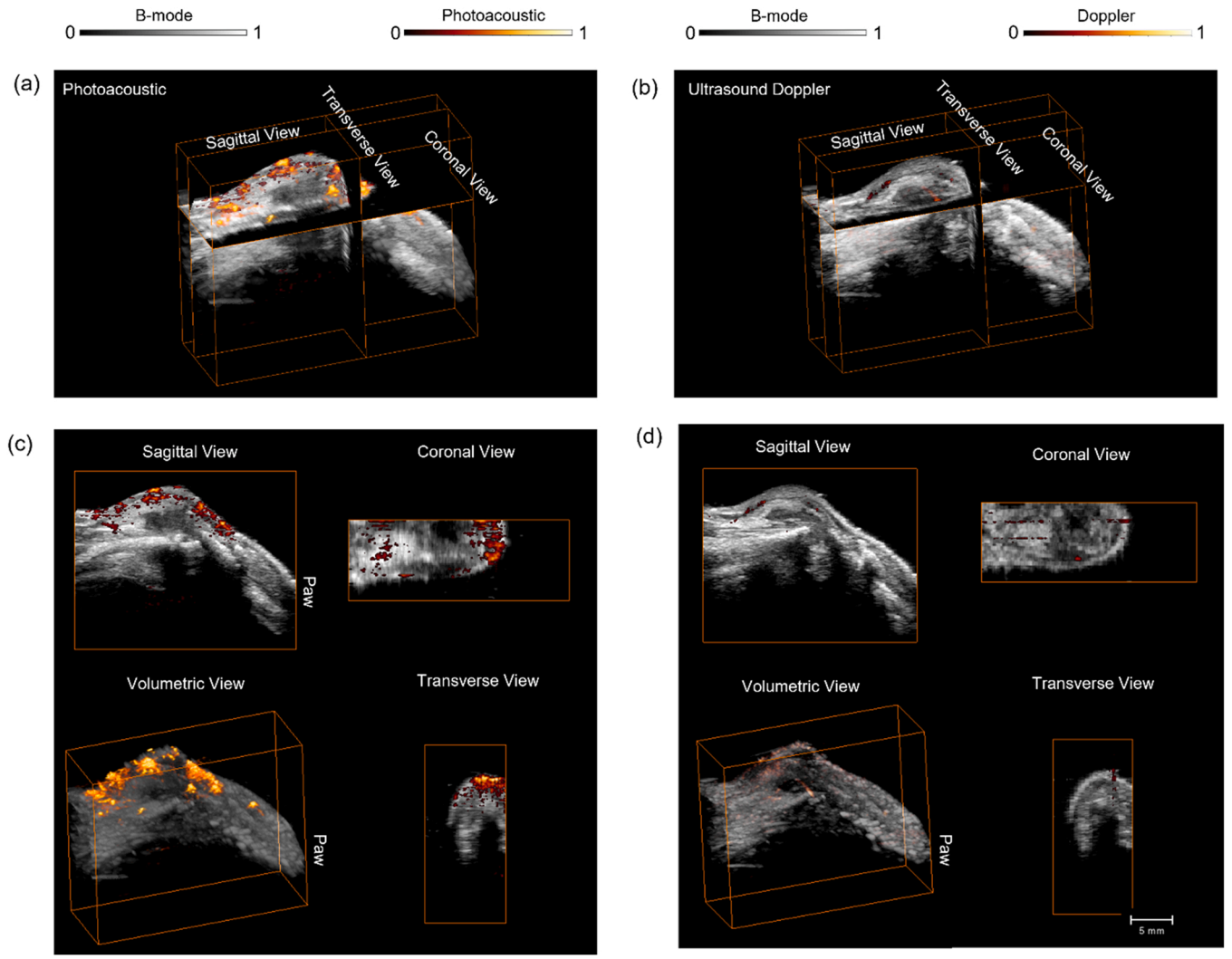

Fig. 6. Volumetric rendering of (a) the 3D B-model US with PA signals and (b) the 3D B-mode US with power Doppler US signals from the arthritis ankle joint acquired on Day 13 after AIA injection. 2D views along three orthogonal planes (coronal, transverse, and sagittal) together with a volumetric view are shown in (c) and (d) for the PA and the power Doppler US results, respectively.

The PA signal in the joint started to increase on Day 11. The increase in power Doppler US signals did not start until Day 13, and became more obvious on Day 15 and Day 16. PA images presented enhanced blood volume (i.e., hyperemia) in the synovial and adjacent regions, while power Doppler US detected enhanced blood flow in a couple large vessels. This difference is because Doppler US is more sensitive to the fast flow in relatively large vessels.

On Day 16, the rat was euthanized and both legs were harvested for histology analysis. The H&E-stained histology photos along the long-axis of the right ankle joint (the same orientation shown in Fig. 4) and along the short-axis of the left ankle joint are shown in Fig. 5. In these histology photos, we can see hyperplasia of the synovial tissue and infiltration of inflammatory cells, which confirmed the arthritis development in the ankle joints [35].

Fig. 6 presents the volumetric renderings of the 3D B-mode US image with PA signals and the 3D B-mode US image with power Doppler US signals. These volumetric renderings of the 3D imaging results were generated using the Amira-Avizo software (Thermo Fisher Scientific, Waltham, MA). These images were acquired on Day 13 from the rat ankle joint with the longitudinal results shown in Fig. 4. The spatially distributed hyperemia reflecting joint inflammation is clearly presented in the 3D PA image in Fig. 6(a). In the 3D power Doppler US image in Fig. 6(b), we can also see active signals reflecting inflammation, and most of the signals are from the large vessels right beneath the skin. Fig. 6(c) and Fig. 6(d) also show the PA and the power Doppler US imaging results along the three orthogonal planes, including coronal, transverse, and sagittal. With these 3D rendering and 2D views of the PA image fused with the high-quality B-mode US image presenting the morphology of the joint, we can see the spatially distributed inflammation in the synovium and surrounding tissues and their relative locations to bones, muscles, and skin.

With the longitudinal 3D imaging results from each joint, we assessed the progress of inflammation by quantifying the hyperemia in the joint, as reflected by both the total intensity of color pixels and the total number of color pixels in the segmented volume in the PA image of the joint. At the same time, we also assessed the progress of inflammation by quantifying the enhanced flow in the joint, as reflected by both the total intensity of color pixels and the total number of color pixels in the same segmented volume in the power Doppler US image of the joint. As mentioned in the Methods section, the total intensity of the color pixels and the total number of color pixels were calculated in the target volume, which was formed by the segmented masks in all the 9 frames.

Fig. 7 shows the quantified results from the 14 joints of the 7 rats. For each joint, the signals were normalized by the maximum value of the PA signals. In each panel showing the result from each joint, the PA curve presenting the change in hyperemia always starts to elevate from the

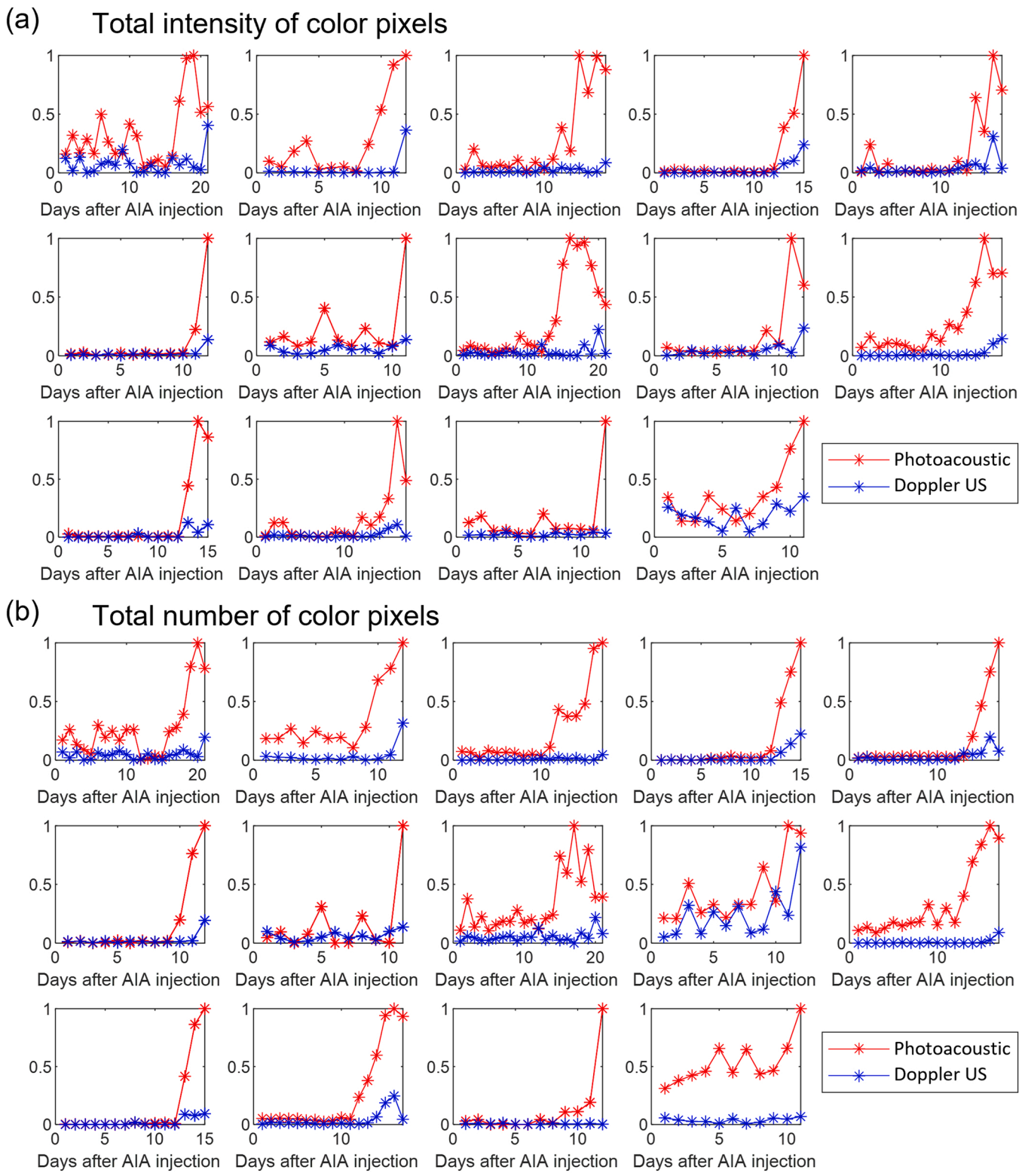

Fig. 7. Longitudinal assessment of joint inflammation by quantifying (a) the total intensity of color pixels and (b) the total number of color pixels in both PA image (red) and power Doppler US image (blue). Each panel shows the measurements from an individual ankle joint, with a total of 14 joints from 7 rats. (For interpretation of the references to color in this figure legend, the reader is referred to the web version of this article.)

baseline earlier than the power Doppler US curve presenting the change in blood flow. This finding from Fig. 7 suggests that PA imaging of hyperemia, quantified either as the total intensity of color pixels or the total number of color pixels in the segmented volume in the joint, is more sensitive in detecting early inflammation when compared to power Doppler US imaging of enhanced blood flow.

With the quantitative measurements from the 14 joints, statistical analyses were performed to evaluate the performance of PA imaging in detecting early arthritis when compared to power Doppler US imaging realized by the same GEHC VE95 US unit. For both PA images and power

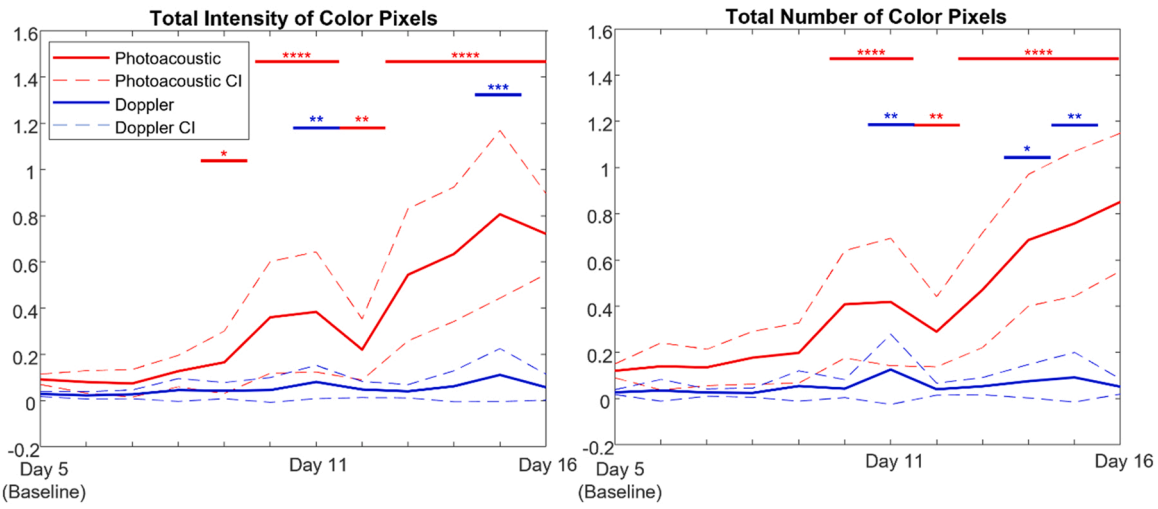

Fig. 8. Statistical analyses to study the longitudinal changes in (a) the total intensity of color pixels and (b) the total number of color pixels in PA images vs. power Doppler US images. On each day, the mean, as shown by the solid curves, and the 95 % confidence intervals (CI), as shown by the dashed curves, are quantified for the measurements from the 14 joints. The data point on each day is compared to the baseline (average of the measurements from 0 to 5 days) via a t-test, and those with statistically significant differences are marked. * ** *: $p < 0.0001$; * ** : $p < 0.001$; * *: $p < 0.01$; * : $p < 0.05$. (For interpretation of the references to color in this figure legend, the reader is referred to the web version of this article.)

Doppler US images, we calculated the average and the 95 % confidence intervals (CI) of the total intensity of color pixels and the total number of color pixels from the 14 joints on each day, as shown in Fig. 8. Considering that no joint inflammation should happen for this AIA model in the very early stage (within a week after AIA injection), we averaged the measurements from Day 0 to Day 5 to generate a baseline, as shown by the measurements on Day 5 in Fig. 8. After Day 5, the mean and the 95% CI are plotted for each day from Day 6 to Day 16. Then the measurement from each day was compared to the baseline value via a t-test, and those with statistically significant differences are marked. The total intensity of color pixels quantified by PA imaging starts to show statistically significant difference from Day 9 ($p < 0.05$ on Day 9 and becomes smaller for later days), while the total intensity of color pixels quantified by power Doppler US imaging exhibits significant difference only on Day 11 and Day 15. The total number of color pixels quantified by PA imaging starts to show statistically significant difference from Day 10 ($p < 0.0001$); while the total number of color pixels quantified by power Doppler US imaging shows significant difference only on Day 11, Day 14, and Day 15. As demonstrated by this statistical study, the hyperemia quantified by PA imaging not only detects joint inflammation earlier than the enhanced blood flow quantified by power Doppler US, but also shows the changes more consistent and robust, as reflected by higher statistical significance.

4. Conclusion and discussion

The performance of our automatic 3D imaging system combining the emerging PA imaging with the conventional Doppler US was examined via a longitudinal study in a clinically relevant AIA rat model. After adjuvant injection, daily imaging of the rat ankle joints was conducted, and the progress in joint inflammation was evaluated by both PA imaging of hyperemia and power Doppler US imaging of enhanced blood flow. As reflected by the imaging results and statistical analyses, although both imaging modalities can detect the inflammation in the joints, PA imaging detects the inflammation earlier in the disease progression and also shows the changes more robustly when compared to power Doppler US, which suggests that, by reflecting the highly sensitive optical contrast, PA imaging is more sensitive to early and mild inflammation associated with arthritis.

Imaging technologies that enable earlier diagnosis and prognosis of arthritis are of great importance in rheumatology clinics as they could enable clinicians to execute the treatment plan before substantial irreversible joint damage occurs. Also, imaging technologies that are sensitive in detecting early treatment response may have significant clinical value as they could enable early treatment modification and personalized medicine, ensuring optimal patient outcome. In this work, we examined the quantified measurements from PA imaging and their changes during the disease progression to understand the clinical value of the emerging PA imaging and benchmarked it against power Doppler US imaging realized by the same commercial grade US unit. This study, in a well-controlled animal model utilizing a well-controlled imaging procedure, facilitated a side-by-side comparison between PA imaging and Doppler US imaging with objective conclusions. As validated in this study, volumetric assessment of inflammation, facilitated by automatic 3D imaging, could lead to a group of robust, reliably reproducible, and precise biomarkers for assessing the progress and severity of arthritis. With the automatic scanning feature, such an imaging device can be handled by any operator without complete medical knowledge (with minimal training), which could lead to better acceptance in rheumatology clinics or resource-limited environments. As a conclusion, the findings from this work suggest that PA imaging, when combined with more established and widely accepted musculoskeletal US imaging, holds potential to change the current procedures in rheumatology clinics.

As demonstrated in previous studies [16,20], PA imaging utilizing multiple laser wavelengths is capable of evaluating soft-tissue hypoxia as another physiological hallmark of arthritis. Multi-wavelength PA imaging, however, was not performed in this study because the aim of this study was the side-by-side comparison between the hyperemia presented by PA imaging and the enhanced blood flow presented by Doppler ultrasound imaging. Currently, PA imaging depth is limited to a few centimeters in most soft tissues. Clinically, this imaging depth is adequate for detecting the inflammation in peripheral joints of human hands and feet. PA imaging of the larger joints in human body, such as knee and hip joints which are also associated with arthritis, is still technically challenging. As another limitation, the segmentation of the synovial tissue and the adjacent region for volumetric analysis of inflammation was achieved manually in this study. Although the manual segmentation with the training and confirmation from board certified rheumatologists and radiologists should be highly accurate, this process is still dependent on the operator. To realize a truly point-of-care imaging system with minimal training requirements, the image

segmentation should also be completed automatically by a computer algorithm. We are currently developing a machine-learning based algorithm for segmentation of synovium in B-mode US images of human finger joints. Once validated, a fully automatic 3D imaging system integrating PA and Doppler US could be achieved, which may eliminate the need for a skilled operator who is experienced in musculoskeletal US.

Declaration of Competing Interest

The authors declare that they have no known competing financial interests or personal relationships that could have appeared to influence the work reported in this paper.

Data availability

Data will be made available on request.

Acknowledgement

This research is supported by the National Institute of Arthritis and Musculoskeletal and Skin Diseases of the National Institute of Health under grant number R01AR060350. The content is solely the responsibility of the authors and does not necessarily represent the official views of the National Institutes of Health.

References

[1] E. Filippucci, E. Cipolletta, R. Mashadi Mirza, M. Carotti, A. Giovagnoni, F. Salaffi, M. Tardella, A. Di Matteo, M. Di Carlo, Ultrasound imaging in rheumatoid arthritis, La Radiol. Med. 124 (11) (2019) 1087–1100.
[2] J.S. Smolen, D.M. Van Der Heijde, E.W. St. Clair, P. Emery, J.M. Bathon, E. Keystone, R.N. Maini, J.R. Kalden, M. Schiff, D. Baker, Predictors of joint damage in patients with early rheumatoid arthritis treated with high-dose methotrexate with or without concomitant infliximab: results from the ASPIRE trial, Arthritis Rheum. 54 (3) (2006) 702–710.
[3] E. Naredo, P. Collado, A. Cruz, M.J. Palop, F. Cabero, P. Richi, L. Carmona, M. Crespo, Longitudinal power Doppler ultrasonographic assessment of joint inflammatory activity in early rheumatoid arthritis: predictive value in disease activity and radiologic progression, Arthritis Care Res. Off. J. Am. Coll. Rheumatol. 57 (1) (2007) 116–124.
[4] M. Dougados, V. Devauchelle-Pensec, J. françois Ferlet, M.-A. D'Agostino, M. Backhaus, J. Bentin, G. Chalès, I. Chary-Valckenaere, P. Conaghan, R. J. Wakefield, The ability of synovitis to predict structural damage in rheumatoid arthritis: a comparative study between clinical examination and ultrasound, Ann. Rheum. Dis. 72 (5) (2013) 665–671.
[5] D. Aletaha, J.S. Smolen, Diagnosis and management of rheumatoid arthritis: a review, Jama 320 (13) (2018) 1360–1372.
[6] E.L. Rowbotham, A.J. Grainger, Rheumatoid arthritis: ultrasound versus MRI, Am. J. Roentgenol. 197 (3) (2011) 541–546.
[7] H. Visser, Early diagnosis of rheumatoid arthritis, Best. Pract. Res. Clin. Rheumatol. 19 (1) (2005) 55–72.
[8] I. Sudoł-Szopińska, L. Jans, J. Teh, Rheumatoid arthritis: what do MRI and ultrasound show, J. Ultrason. 17 (68) (2017) 5.
[9] R. Wakefield, P. O'connor, P. Conaghan, D. McGonagle, E. Hensor, W. Gibbon, C. Brown, P. Emery, Finger tendon disease in untreated early rheumatoid arthritis: a comparison of ultrasound and magnetic resonance imaging, Arthritis Care Res. 57 (7) (2007) 1158–1164.
[10] M. Østergaard, M. Hansen, M. Stoltenberg, I. Lorenzen, Quantitative assessment of the synovial membrane in the rheumatoid wrist: an easily obtained MRI score reflects the synovial volume, Rheumatology 35 (10) (1996) 965–971.
[11] A. Savnik, H. Malmskov, H.S. Thomsen, L.B. Graff, H. Nielsen, B. Danneskiold-Samsøe, J. Boesen, H. Bliddal, MRI of the wrist and finger joints in inflammatory joint diseases at 1-year interval: MRI features to predict bone erosions, Eur. Radiol. 12 (5) (2002) 1203–1210.
[12] M. Østergaard, M. Stoltenberg, P. Løvgreen-Nielsen, B. Volck, C.H. Jensen, I. Lorenzen, Magnetic resonance imaging-determined synovial membrane and joint effusion volumes in rheumatoid arthritis and osteoarthritis. Comparison with the macroscopic and microscopic appearance of the synovium, Arthritis Rheum. 40 (10) (1997) 1856–1867.
[13] M. Backhaus, T. Kamradt, D. Sandrock, D. Loreck, J. Fritz, K. Wolf, H. Raber, B. Hamm, G.R. Burmester, M. Bollow, Arthritis of the finger joints: a comprehensive approach comparing conventional radiography, scintigraphy, ultrasound, and contrast-enhanced magnetic resonance imaging, Arthritis Rheum. Off. J. Am. Coll. Rheumatol. 42 (6) (1999) 1232–1245.
[14] R.J. Wakefield, W.W. Gibbon, P.G. Conaghan, P. O'Connor, D. McGonagle, C. Pease, M.J. Green, D.J. Veale, J.D. Isaacs, P. Emery, The value of sonography in the detection of bone erosions in patients with rheumatoid arthritis: a comparison with conventional radiography, Arthritis Rheum. 43 (12) (2000) 2762–2770.
[15] M. Magnani, E. Salizzoni, R. Mule, M. Fusconi, R. Meliconi, S. Galletti, Ultrasonography detection of early bone erosions in the metacarpophalangeal joints of patients with rheumatoid arthritis, Clin. Exp. Rheumatol. 22 (6) (2004) 743–748.
[16] J. Jo, G. Xu, M. Cao, A. Marquardt, S. Francis, G. Gandikota, X. Wang, A functional study of human inflammatory arthritis using photoacoustic imaging, Sci. Rep. 7 (1) (2017) 15026.
[17] J. Jo, G. Xu, Y. Zhu, M. Burton, J. Sarazin, E. Schiopu, G. Gandikota, X. Wang, Detecting joint inflammation by an LED-based photoacoustic imaging system: a feasibility study, J. Biomed. Opt. 23 (11) (2018) 1–4.
[18] J. Jo, G. Xu, E. Schiopu, D. Chamberland, G. Gandikota, X. Wang, Imaging of enthesitis by an LED-based photoacoustic system, J. Biomed. Opt. 25 (2020) 12.
[19] C. Zhao, Q. Wang, X. Tao, M. Wang, C. Yu, S. Liu, M. Li, X. Tian, Z. Qi, J. Li, F. Yang, L. Zhu, X. He, X. Zeng, Y. Jiang, M. Yang, Multimodal photoacoustic/ultrasonic imaging system: a promising imaging method for the evaluation of disease activity in rheumatoid arthritis, Eur. Radiol. 31 (5) (2021) 3542–3552.
[20] M. Yang, C. Zhao, M. Wang, Q. Wang, R. Zhang, W. Bai, J. Liu, S. Zhang, D. Xu, S. Liu, X. Li, Z. Qi, F. Yang, L. Zhu, X. He, X. Tian, X. Zeng, J. Li, Y. Jiang, Synovial oxygenation at photoacoustic imaging to assess rheumatoid arthritis disease activity, Radiology 306 (1) (2023) 220–228.
[21] J. Jo, G. Xu, Y. Zhu, M. Burton, J. Sarazin, E. Schiopu, G. Gandikota, X. Wang, Detecting joint inflammation by an LED-based photoacoustic imaging system: a feasibility study, J. Biomed. Opt. 23 (11) (2018), 110501-110501.
[22] J.R. Rajian, G. Girish, X. Wang, Photoacoustic tomography to identify inflammatory arthritis, J. Biomed. Opt. 17 (9) (2012), 96013-96011.
[23] J.R. Rajian, X. Shao, D.L. Chamberland, X. Wang, Characterization and treatment monitoring of inflammatory arthritis by photoacoustic imaging: a study on adjuvant-induced arthritis rat model, Biomed. Opt. Express 4 (6) (2013) 900–908.
[24] D.L. Chamberland, X. Wang, B.J. Roessler, Photoacoustic tomography of carrageenan-induced arthritis in a rat model, J. Biomed. Opt. 13 (1) (2008), 011005.
[25] D.L. Chamberland, J.D. Taurog, J.A. Richardson, X. Wang, Photoacoustic tomography: a new imaging technology for inflammatory arthritis - as applied to tail spondylitis in rats, Clin. Exp. Rheuma 27 (2) (2009) 387–388.
[26] S. Shahrara, A.E. Proudfoot, J.M. Woods, J.H. Ruth, M.A. Amin, C.C. Park, C. S. Haas, R.M. Pope, G.K. Haines, Y.Y. Zha, A.E. Koch, Amelioration of rat adjuvant-induced arthritis by Met-RANTES, Arthritis Rheum. 52 (6) (2005) 1907–1919.
[27] Y. Lin, S. Xiao, W. Yao, Z. Lv, Y. Tang, Y. Zhang, L. Chen, Molecular photoacoustic imaging for early diagnosis and treatment monitoring of rheumatoid arthritis in a mouse model, Am. J. Transl. Res. 13 (8) (2021) 8873–8884.
[28] Ogawa, K., Namita, T., Kondo, K., Yamakawa, M., Evaluation of arthritis with model rats using photoacoustic imaging system', in Editor (Ed.)'(Eds.), 'Book Evaluation of Arthritis with Model Rats Using Photoacoustic Imaging System, 2019 ed., Optica Publishing Group, 2019, 11077_11055.
[29] A.E. Koch, The role of angiogenesis in rheumatoid arthritis: recent developments, Ann. Rheum. Dis. 59 (Suppl 1) (2000) i65–i71.
[30] E. Bodolay, A.E. Koch, J. Kim, G. Szegedi, Z. Szekanecz, Angiogenesis and chemokines in rheumatoid arthritis and other systemic inflammatory rheumatic diseases, J. Cell Mol. Med. 6 (3) (2002) 357–376.
[31] A.E. Koch, Angiogenesis as a target in rheumatoid arthritis, Ann. Rheum. Dis. 62 (Suppl 2) (2003) ii60–ii67.
[32] J.D. Taurog, D.C. Argentieri, R.A. McReynolds, Adjuvant arthritis, Methods Enzym. 162 (1988) 339–355.
[33] S. Hayer, M.J. Vervoordeldonk, M.C. Denis, M. Armaka, M. Hoffmann, J. Bäcklund, K.S. Nandakumar, B. Niederreiter, C. Geka, A. Fischer, SMASH'recommendations for standardised microscopic arthritis scoring of histological sections from inflammatory arthritis animal models, Ann. Rheum. Dis. 80 (6) (2021) 714–726.
[34] R. Pan, Y. Dai, X. Gao, Y. Xia, Scopolin isolated from Erycibe obtusifolia Benth stems suppresses adjuvant-induced rat arthritis by inhibiting inflammation and angiogenesis, Int. Immunopharmacol. 9 (7–8) (2009) 859–869.
[35] T. Nakasa, S. Miyaki, A. Okubo, M. Hashimoto, K. Nishida, M. Ochi, H. Asahara, Expression of microRNA-146 in rheumatoid arthritis synovial tissue, Arthritis Rheum. 58 (5) (2008) 1284–1292.

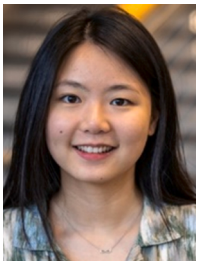

Xiaorui Peng received her B.S. degree in Electrical Engineering from Beijing Institute of Technology in 2019 and her master's degree in Biomedical Engineering from Duke University in 2021. Now, Xiaorui joined the Optical Imaging Laboratory and is pursuing her Ph.D. degree in Biomedical Engineering at the University of Michigan. Her current research interests focus on potential clinical applications of photoacoutics.

Zhanpeng Xu is a Ph.D. candidate from the Department of Biomedical Engineering, University of Michigan, Ann Arbor. He received his B.S. degree from Sichuan University and M.S. degree from Zhejiang University in China. His research interests focus on photoacoustic measurement and imaging, photoacoustic microscopy, hyperspectral imaging et al. He has published more than 10 peer-reviewed journal papers, and served as the independent reviewer for Optics Express, Optics Letters, Biomedical Optics Express, Progress in Electromagnetics Research, Applied Optics, and Plos One.

Aaron Dentinger received his B.S. degree in engineering physics in 1992 and his M. S. and Ph.D. degrees in electrical engineering in 1994 and 2006, respectively, from Rensselaer Polytechnic Institute, Troy, NY., Since 1995, he has worked as an Electrical Engineer at GE Global Research in Niskayuna, NY and is currently a member of the Ultrasound and Biomedical Laboratory. Prior to joining GE, he was employed at Reveo, Inc. His current research interests are in ultrasound signal and image processing for vascular, cardiac, and physiological measurements.

Shivangi Kewalramani received her B.E. degree in Electronics and Communications from Birla Institute of Technology and Science, Dubai in 2019 and is pursuing a master's degree in Biomedical Engineering along with minor's in Data Science from University of Michigan. She has carried out research on photoacoustic imaging in the optical engineering area.

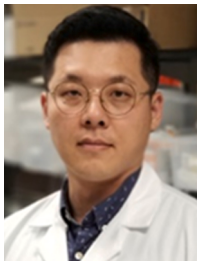

Janggun Jo received his B.S. and M.S. degree in Electronic Engineering from KoreaTech in Korea. He received his Ph.D. degree in Bioengineering at the University of Kansas. And Dr. Jo finished his postdoc fellowship at the University of Michigan. Currently he is a Research Investigator in the Department of Biomedical Engineering at the University of Michigan. His research interests include Photoacoustic imaging modality including Optical and Ultrasound imaging as well as high intensity focused ultrasound treatment.

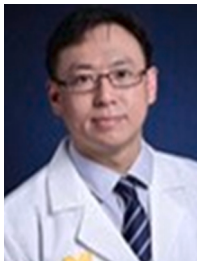

Guan Xu received his PhD and postdoctoral training in optical and ultrasound imaging in biomedicine. He received a predoctoral award from Congressionally Directed Medical Research Programs, a postdoctoral fellowship from American Heart Association, a Career Development Award from American Gastroenterology Association, a Senior Research Award from Crohn's and Colitis Foundation and an R37 MERIT award from National Cancer Institute.

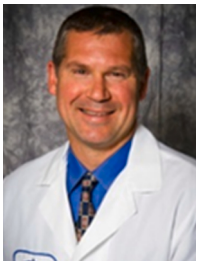

David Chamberland received his B.S. in Electrical Engineering from the University of Portland and his M.D. from the Oregon Health Sciences University. He joined the University of Michigan in 2004 and has been working on medical applications of photoacoustic technology for over 15 years. His training in electrical engineering and also a long history of working as a clinical rheumatologist with board certifications in internal medicine and rheumatology enable him to help with translation of applications into the clinical space.

Nada Abdulaziz received her medical degree from the University of Khartoum Faculty of Medicine. Her followship in Rheumatology was at the University of Michigan, where she pursued her career as Clinical assistant professor in Rheumatology Division. As a faculty member, she has been awarded W. J. (Joe) McCune Award for Teaching Excellence. She is currently a member in the fellowship Competency Committees that oversee the academic progression of rheumatology fellows across all phases of their training. She has an interest in inflammatory myositis diseases and is part of a multidisciplinary team in myositis program.

Girish Gandikota obtained board certifications in surgery (F.R.C.S.) and Radiology (F.R.C.R.) in the U.K. He did his fellowship in Musculoskeletal Radiology at McMaster University, Hamilton, Ontario, Canada. After the fellowship, he joined the University of Michigan as a lecturer. He has been promoted successfully to the professor and has received American board certification (A.B.R.). He has also obtained ultrasound R.M.S.K. certification from APCA/ARDMS. Winner of the excellence in teaching awards, Dr. Gandikota has been an invited speaker, delivering more than 300 invited lectures and national presentations. He has over 75 scientific papers/exhibits in national conferences and over 68 peer-reviewed publications to date. His main research interests include M.S.K. Ultrasound, Sports Medicine, and Arthritis. Presently has over 15 years of M.S.K. ultrasound experience. Conducts C.M.E. courses on M.S.K. radiology and ultrasound in U.S.A. and India. He is a co-investigator in a NIH RO1 Grant ($3,545,507) on Arthritis. He has mentored many residents, fellows, technologists and medical students. Dr. Gandikota recently joined us from the University of Michigan where he was Professor of Radiology. In addition to teaching and research, Dr. Gandikota had multiple administrative roles at the University of Michigan and at the national level. He was the Chair of Clinical Competency Committee, Radiology Residency Program, and in charge of M.S.K. resident training, curriculum development, and evaluation. He was also the Director, Domino Farms Radiology. He is a member of national professional societies like the Radiological Society of North America (R.S.N.A.), American Roentgen Ray Society (A.R.R.S.), Society of Skeletal Radiology (S.S.R.), and American Institute of Ultrasound in Medicine (A.I.U.M.), where he regularly lectures. He was the Chair of the Assessment Oversight Team (A.O.T.) RMSK-APCA appointed for the musculoskeletal physician examination. He is a reviewer for multiple esteemed radiology and rheumatology journals, including Arthritis and rheumatology.

David Mills is a Principal Scientist in the Ultrasound and Bioinstrumentation lab at GE Research in Niskayuna, NY. He received the B.S. degree in engineering (summa cum laude) from LeTourneau University, Longview, TX, USA, in 1994, and the Ph.D. degree in biomedical engineering from Duke University, Durham, NC, USA, in 2000. He joined GE Research in 2000 where he is involved in the research and development of medical ultrasound transducers and advanced ultrasound applications. He has led multiyear research programs on ultrasound applications and drug delivery using microbubbles, including scan guidance and image analysis technology. He has authored many publications and conference presentations in these areas and holds more than 25 patents related to medical ultrasound. His current research interests include the design of medical ultrasound transducers of both piezoelectric and cMUT-based transducers and new clinical applications for ultrasound that are enabled by real-time 3-D ultrasound imaging, visualization algorithms, and customized user interfaces to meet specific user needs.

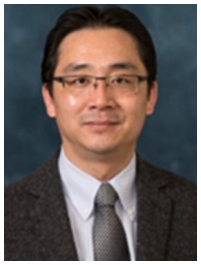

Xueding Wang is a Jonathan Rubin Collegiate Professor of the Department of Biomedical Engineering and the Professor of the Department of Radiology at the University of Michigan School of Medicine. Before working as an independent principal investigator, Dr. Wang received his Ph.D. at Texas A&M University and Postdoctoral training at the University of Michigan. Dr. Wang has extensive experience in development of medical imaging and treatment technologies, especially those involving light and ultrasound. Sponsored by NIH, NSF, DoD and other funding agencies, his research has led to over 160 + peer-reviewed journal papers. Dr. Wang was the recipient of the Sontag Foundation Fellow of the Arthritis National Research Foundation in 2005, the Distinguished Investigator Award of the Academy of Radiology Research in 2013, and was elected to the fellow of AIMBE in 2020 and the fellow of SPIE in 2021. He is also sitting on the editorial boards of scientific journals including Photoacoustics, Ultrasonic Imaging, Journal of Biomedical Optics, Medical Physics, and Scientific Reports.